

Generic Contrast Agents

Our portfolio is growing to serve you better. Now you have a *choice*.



[VIEW CATALOG](#)

AJNR

High-Resolution MR Cisternography of the Cerebellopontine Angle, Obtained with a Three-Dimensional Fast Asymmetric Spin-Echo Sequence in a 0.35-T Open MR Imaging Unit

Shinji Naganawa, Tokiko Ito, Eriko Iwayama, Hiroshi Fukatsu and Takeo Ishigaki

This information is current as of May 9, 2025.

AJNR Am J Neuroradiol 1999, 20 (6) 1143-1147
<http://www.ajnr.org/content/20/6/1143>

High-Resolution MR Cisternography of the Cerebellopontine Angle, Obtained with a Three-Dimensional Fast Asymmetric Spin-Echo Sequence in a 0.35-T Open MR Imaging Unit

Shinji Naganawa, Tokiko Ito, Eriko Iwayama, Hiroshi Fukatsu, and Takeo Ishigaki

Summary: High-resolution MR cisternography performed with 3D fast asymmetric spin-echo imaging (3D fast spin-echo with an ultra-long echo train length and asymmetric Fourier imaging) was optimized in a 0.35-T open MR imaging unit. The 0.35- and 1.5-T images of the two volunteers and three patients with acoustic schwannomas were then compared. The optimal parameters for images obtained by 3D fast asymmetric spin-echo imaging at 0.35 T were as follows: field of view, 15 cm; matrix, $256 \times 256 \times 40$; section thickness, 1 mm; echo train length, 76; and imaging time, 10 minutes 44 seconds. Scans obtained from both normal volunteers showed the facial, cochlear, and superior and inferior vestibular nerves separately in the internal auditory canal on both 0.35- and 1.5-T images. All three acoustic schwannomas were depicted on both 0.35- and 1.5-T images. Screening for disease at the cerebellopontine angle and in the internal auditory canal, without the administration of contrast material on a low-field open MR imaging unit and within a clinically acceptable imaging time, may be possible. Further controlled prospective studies are required, however, before implementation on a wide basis. If proved effective, this may be of particular value for reducing healthcare costs and for imaging claustrophobic and pediatric patients in an open system.

Open MR imaging units are becoming more widespread, and are frequently used for MR-guided interventional procedures for the comfort of claustrophobic and pediatric patients, and for major joint movement studies. Nonetheless, most of a unit's operating time is spent performing routine MR imaging studies. Even with open units, high-resolution images are desirable for studies such as screening for acoustic schwannomas in the cerebellopontine angle and internal auditory canal. The clinical val-

ue of high-resolution heavily T2-weighted MR imaging of the inner ear and cerebellopontine angle, using 2D fast spin-echo (1), 3D constructive interference in steady state (2), and 3D fast spin-echo (3–8) imaging recently has been reported for high-field magnets. Three-dimensional fast spin-echo imaging with an ultra-long echo train length and asymmetric Fourier imaging (3D fast asymmetric spin-echo) has been developed, optimized, and evaluated clinically at 1.5 T (4). In this study, a 3D fast spin-echo sequence was optimized on a 0.35-T open MR imaging unit. The 0.35- and 1.5-T images of two normal volunteers and three patients with acoustic schwannomas in the cerebellopontine angle or internal auditory canal were compared.

Patients and Methods

All images were obtained on a 0.35-T open scanner (Opact; Toshiba America, San Francisco, CA) and on a 1.5-T scanner (Visart; Toshiba, Tokyo, Japan). A quadrature head coil was used for all experiments, at both 0.35 and 1.5 T.

Five participants underwent imaging for optimization of the 3D fast asymmetric spin-echo pulse sequence (experiments 1–4). The following parameters were used for all experiments at 0.35 T: axial single section; field of view, 15 cm; matrix, $256 \times 256 \times 40$; section thickness, 1 mm; echo spacing, 20 milliseconds; and imaging time, 10 minutes 44 seconds. Two radiologists evaluated qualitatively the appearance of anatomic structures (the facial nerve, cochlear nerve, superior vestibular nerve, inferior vestibular nerve, cochlear turns, vestibule, and three semicircular canals), degree of blur on images, and ghost artifacts on source images. Two radiologists separately scored the images as excellent (score of 3), good (score of 2), fair (score of 1), and poor (score of 0). If there were any discrepancies, consensus was obtained by discussion. The contrast-to-noise ratio values between the CSF and the cerebellar peduncle were compared quantitatively on source images.

Experiments for Parameter Optimization

The number of shots, which determines the echo train length, varied from one to four. The number of shots consists of the number of excitation pulses used to cover the x - y plane of the k -space for one section-encoding step. The parameters were varied as follows: one shot, 140 echo train length with 4 excitations; two shots, 76 echo train length with 2 excitations; and four shots, 44 echo train length with 1 excitation at 4000 (TR). Images obtained with the parameters of 4000/2 (TR/excitations), 8000/1, 120/180/240 (TE/TE/TE), and with and

Received July 19, 1998; accepted after revision, November 4, 1998.

Presented at the sixth meeting of the International Society of Magnetic Resonance in Medicine at Sydney, Australia, in April 1998.

From the Department of Radiology, Nagoya University School of Medicine, Nagoya, Japan.

Address reprint requests to Shinji Naganawa, MD, Department of Radiology, Nagoya University School of Medicine, 65 Tsurumai-cho, Showa-ku, Nagoya, 466-8550 Japan.

© American Society of Neuroradiology

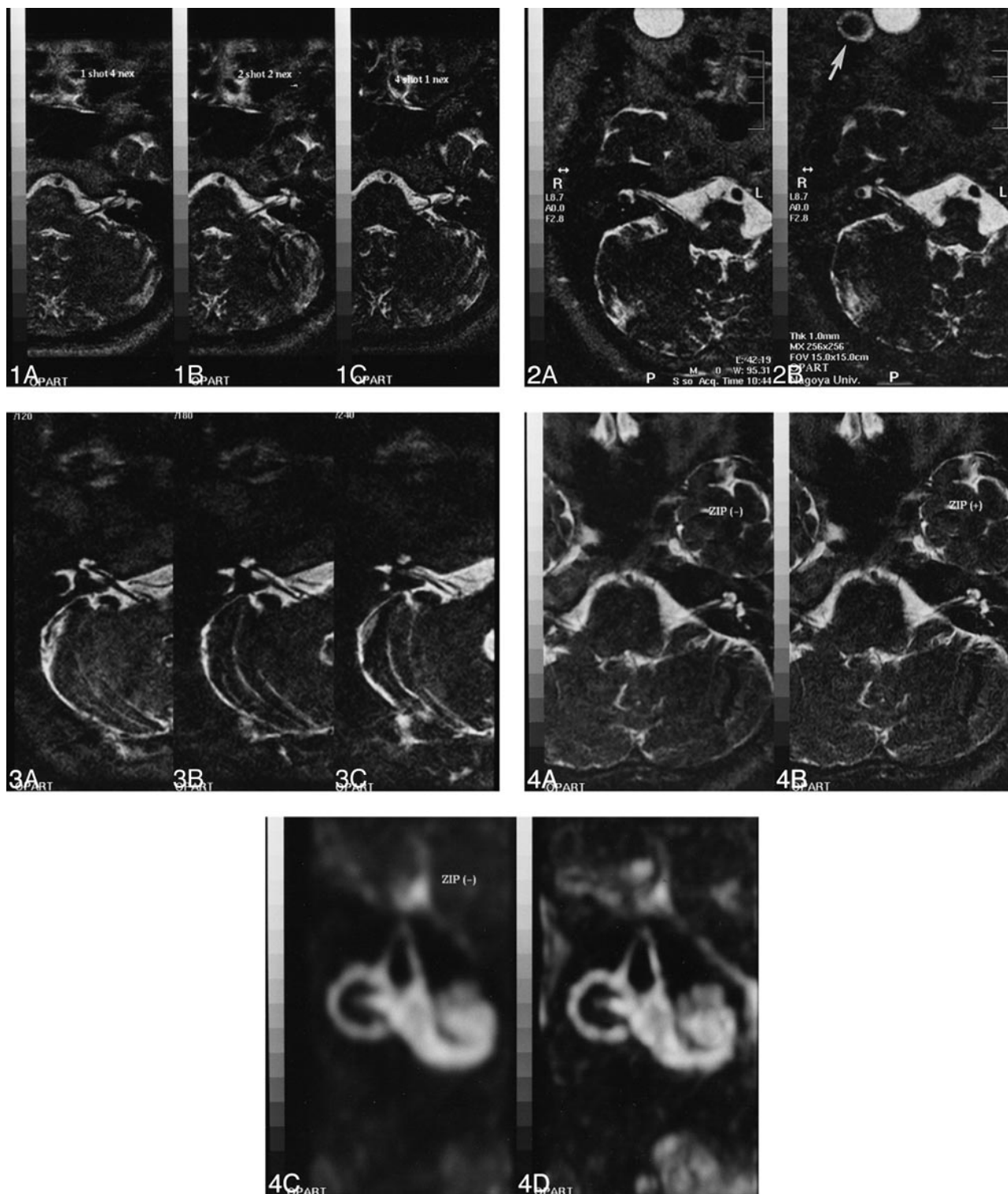


FIG 1. Comparisons of the images obtained in different numbers of shots. The images obtained in one shot (A) showed contrast-to-noise ratio values that were comparable with those obtained in two shots (B); however, they showed more blur. The images obtained in four shots showed the lowest contrast-to-noise ratio values with the least degree of blur (C).

A, One shot; echo train length, 140; number of excitations, 4.

B, Two shots; echo train length, 76; number of excitations, 2.

C, Four shots, echo train length, 44; 4000/240/1 (TR/TE/excitations); field of view, 15 cm; matrix, $256 \times 256 \times 40$; section thickness, 1 mm; echo spacing, 20 milliseconds; and imaging time, 10 minutes 44 seconds.

FIG 2. Comparisons of the images with different TRs. Images with 4000/2 (TR/excitations) (A) and 8000/1 (B) showed comparable contrast-to-noise ratio values. Images with 8000/1 showed some ghost artifacts (arrow). Other parameters are the same for both TRs: two shots; echo train length, 76; 240 (TE); field of view, 15 cm; matrix, $256 \times 256 \times 40$; section thickness, 1 mm; echo spacing, 20 milliseconds; and imaging time, 10 minutes 44 seconds.

FIG 3. Comparisons of the images with 120 (TE) (A), 180 (B), and 240 (C). Images with 240 showed the best contrast-to-noise ratio

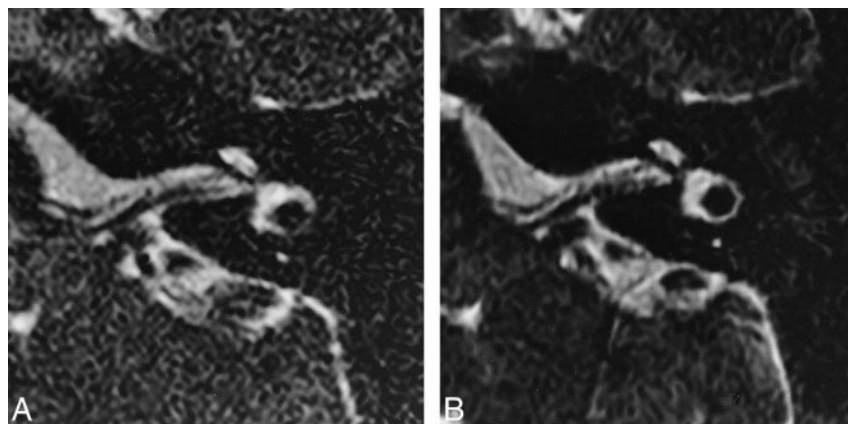


FIG 5. Images obtained at 1.5 T (imaging time, 3 minutes) (A) and 0.35 T (imaging time, 11 minutes) (B) provided comparable anatomic information.

A, The imaging parameters at 1.5 T were as follows: field of view, 15 cm; section thickness, 1 mm; 5000/250/1 (TR/TE/excitations); one shot; echo train length, 148; matrix, $256 \times 256 \times 30$, which zero-filled to $512 \times 512 \times 60$; echo spacing, 12.5 milliseconds; and imaging time, 2 minutes 45 seconds.

B, The imaging parameters for 0.35 T were as follows: field of view, 15 cm; section thickness, 1 mm; 4000/240/2; two shots; echo train length, 76; matrix, $256 \times 256 \times 40$, which zero-filled to $512 \times 512 \times 80$; and imaging time, 10 minutes 44 seconds.

without zero-fill interpolation were compared. Images were obtained at 4000/240/2 (TR/TE/number of excitations) in two shots in 10 minutes 44 seconds.

Comparison of 0.35- and 1.5-T Images

Images obtained at 1.5 and 0.35 T were compared qualitatively as in the experiments for parameter optimization. For the two normal volunteers, the parameters at 1.5 T were as follows: field of view, 15 cm; section thickness, 1 mm; 5000/250/1 (TR/TE/excitations); one shot; echo train length, 148; matrix, $256 \times 256 \times 30$, which zero-filled to $512 \times 512 \times 60$; echo spacing, 12.5 milliseconds; and imaging time, 2 minutes 45 seconds. This is a previously reported routine protocol for the screening of acoustic schwannomas on the same 1.5-T MR scanner (4). The imaging parameters for 0.35 T were as follows: field of view, 15 cm; section thickness, 1 mm; 4000/240/2; two shots; echo train length, 76; matrix, $256 \times 256 \times 40$, which zero-filled to $512 \times 512 \times 80$; and imaging time, 10 minutes 44 seconds. Three patients with known acoustic schwannomas (2, 6, and 12 mm in size) underwent 0.35- and 1.5-T imaging.

The imaging parameters for scans obtained at 1.5-T were the same for those used for two patients with schwannomas as those used for the two volunteers. Imaging times used for 1.5-T scans obtained from the remaining patient, however, were made similar to those times obtained at 0.35 T. This was performed to evaluate image quality obtained from 1.5-T images at alternative imaging times. The scanning parameters for this patient imaged at 1.5 T were as follows: field of view, 16 cm; section thickness, 0.8 mm; 4000/240 (TR/TE); four shots; echo train length, 79; matrix, $512 \times 512 \times 40$; echo spacing, 15.0 milliseconds; and imaging time, 11 minutes 48 seconds. The imaging parameters for the 0.35-T images were the same as those for the two normal volunteers and the two other patients. The appearance of the acoustic schwannomas on the images obtained at 0.35 and 1.5 T were compared qualitatively. Two radiologists separately graded the delineation of the tumor as excellent (score of 3), good (score of 2), fair (score of 1), or poor (score of 0). They were not blinded to the side of the acoustic schwannoma.

Results

Experiments for Parameter Optimization

The images acquired in one shot showed contrast-to-noise ratio values (contrast-to-noise ratio = 13.0) that were comparable with those acquired in two shots (contrast-to-noise ratio = 15.0); however, those obtained in one shot had a more blurred appearance. The average score (\pm standard deviation) among five participants was 2.2 ± 0.4 for one shot, 2.8 ± 0.4 for two shots, and 2.0 ± 0.0 for four shots. The images acquired in four shots showed the lowest contrast-to-noise ratio values (contrast-to-noise ratio = 8.9) with slightly less blur than those acquired in two shots (Fig 1). All of the images delineated all anatomic structures, regardless of number of shots. Images with 4000/2 (TR/excitations) and 8000/1 showed comparable contrast-to-noise ratio values (contrast-to-noise ratio: 4000 = 15.7, 8000 = 16.3). Images with 8000/1 showed some ghost artifacts (Fig 2). The average score was 2.8 ± 0.4 for those with TRs of 4000 and 2.4 ± 0.5 for those with 8000. The images with both TRs depicted all anatomic structures. Images with TEs of 240 showed the best contrast-to-noise ratio (Fig 3) (contrast-to-noise ratio: 120 = 7.4, 180 = 16.9, 240 = 19.1). The average score was 1.8 ± 0.4 for TEs of 120, 2.4 ± 0.5 for those with 180, and 2.8 ± 0.4 for those with 240. All of the images showed all anatomic structures, regardless of TE. Images with zero-fill interpolation showed less blur on both source images and maximum intensity projection images of the labyrinth (Fig 4). The average score was 2.8 ± 0.4 for both images.

values. Other parameters were the same for all TEs: two shots; 4000 (TR); field of view, 15 cm; matrix, $256 \times 256 \times 40$; section thickness, 1 mm; echo spacing, 20 milliseconds; and imaging time, 10 minutes 44 seconds.

FIG 4. Images without zero-fill interpolation showed more blur on both source images (A) and maximum intensity projection images (C) of the labyrinth than on those with ZIP¹ (B and D). The imaging parameters were as follows: field of view, 15 cm; section thickness, 1 mm; 4000/240/2 (TR/TE/excitations); two shots; echo train length, 76; matrix, $256 \times 256 \times 40$, which zero-filled to $512 \times 512 \times 80$; and imaging time, 10 minutes 44 seconds.

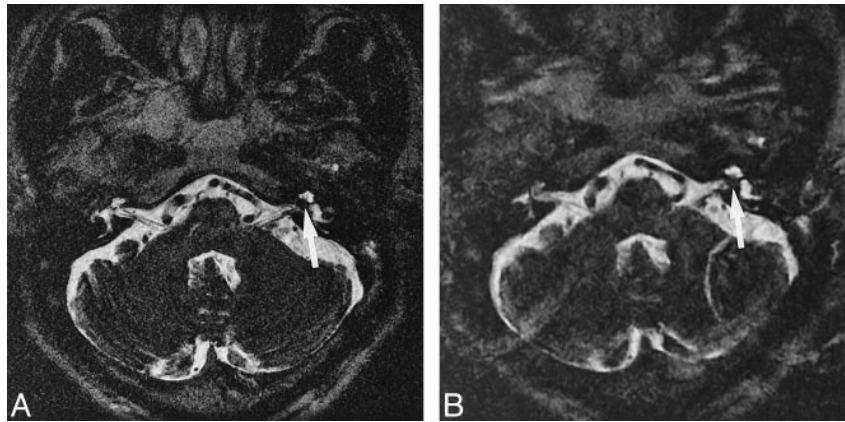


FIG 6. A case of a 2-mm intracanalicular acoustic schwannoma. A small filling defect in the CSF of the left internal auditory canal was depicted on both 1.5-T images (imaging time, 12 minutes) (A) and 0.35-T images (imaging time, 11 minutes) (B) (arrows).

A, The imaging parameters at 1.5 T were as follows: field of view, 16 cm; section thickness, 0.8 mm; 4000/240 (TR/TE); four shots; echo train length, 79; matrix, $512 \times 512 \times 40$; echo spacing, 15.0 milliseconds; and imaging time, 11 minutes 48 seconds.

B, The imaging parameters for 0.35 T were the same as those presented in the legend to Figure 5B. Our protocol for "the screening brain and internal auditory canal" included T2-weighted images for whole-brain and MR cisternography with 3D fast asymmetry spin-echo images obtained in 2 minutes 45 seconds. The protocol for "screening internal auditory canal only" for the patients who had finished their whole-brain study was MR cisternography with 3D fast asymmetric spin-echo images obtained in 12 minutes. For this image, the latter protocol was applied to compare the image quality between the 0.35- and 1.5-T images obtained during comparable imaging time. Note the considerable difference in the image quality between the 0.35- and 1.5-T images when obtained during comparable imaging time, although the pathologic findings can be appreciated on either image.

Comparison of 0.35- and 1.5-T Images

Images obtained at 1.5 and 0.35 T delineated the same anatomic structures in the two volunteers (Fig. 5). Images obtained from the normal volunteers depicted the facial, cochlear, and superior and inferior vestibular nerves separately in the internal auditory canal at both 0.35 and 1.5 T (Score = 3 for all images).

Although the images obtained at 1.5 T in 12 minutes provided clearer delineation of the tumor than those obtained at 0.35 T in 11 minutes, all three acoustic schwannomas were depicted on both 0.35- and 1.5-T images (Fig. 6). The score was 3 for all images obtained at 1.5 T, and the scores were 3, 2, and 2 for those obtained at 0.35 T.

Discussion

The low, mid-field, open MR imaging units are being used more frequently because of the pressure to achieve healthcare cost reduction and the need for patient comfort during examination. Generally, these open units are not suitable for high-resolution imaging. Even with fast imaging, the imaging time has to be set longer compared with 1.5-T imaging. This difference in output between 0.35 and 1.5 T is an important issue. For example, the necessary time for T1- and T2-weighted imaging for whole-brain MR cisternography using 3D fast asymmetric spin-echo, patient setup, and preimaging would be approximately 20 minutes at 1.5 T, but 30 minutes at 0.35 T. This may reduce the cost efficiency and time efficiency at 0.35 T.

The screening protocol for imaging the internal auditory canal with 3D fast asymmetric spin-echo needs to be confirmed by the contrast-enhanced T1-

weighted images, even at 1.5 T, when the internal auditory canal is narrow or its walls irregular. With the former, delineation of its four nerves can be obscured, and with the latter, imaging may erroneously show a filling defect of CSF (5). At 0.35 T, the number of this kind of "false positive" cases would increase compared with 1.5 T because of a lower signal-to-noise ratio and limited spatial resolution. This also reduces the efficiency of the screening protocol at 0.35 T.

In this study, a quadrature head coil was used at both magnetizations; however, a dedicated phased-array receiver, if available, would enhance the image quality (1, 4, 5). This preliminary study suggested the efficacy of MR cisternography, performed at 0.35 T and without administration of contrast material, for the screening of small intracanalicular acoustic schwannomas. Nevertheless, the sensitivity and specificity of unenhanced MR cisternography performed at 0.35 T for the diagnosis of acoustic schwannoma should be evaluated by a prospective study comparing this technique with conventional contrast-enhanced MR imaging.

Conclusion

MR cisternography performed with 3D fast asymmetric spin-echo imaging is possible. Screening for pathologic lesions performed at the cerebellopontine angle and in the internal auditory canal, without the administration of contrast material, on a low-field open MR imaging unit, and within a clinically acceptable imaging time may be possible. Nevertheless, further controlled prospective studies are required before its implementation on a wide basis. If proved effective, this may be of par-

ticular value for reducing healthcare costs, and for imaging claustrophobic and pediatric patients in an open system.

References

1. Allen RW, Harnsberger HR, Shelton C, et al. **Low-cost high-resolution fast spin-echo MR of acoustic schwannoma. An alternative to enhanced conventional spin-echo MR?** *AJNR Am J Neuroradiol* 1996;17:1205–1210
2. Hermans R, Goten AV, De Foer B, Baert AL. **MRI screening for acoustic neuroma without gadolinium. Value of 3DFT-CISS sequence.** *Neuroradiology* 1997;39:593–598
3. Naganawa S, Yamakawa K, Fukatsu H, et al. **High-resolution T2-weighted MR imaging of the inner ear using a long echo-train-length 3D fast spin-echo sequence.** *Eur Radiol* 1996;6:369–374
4. Takehara Y, Ichijyo K, Tooyama N, et al. **Three-dimensional projection images of the labyrinth acquired with multislab 3DFT fast spin-echo sequence and dual-array surface coil.** *AJR Am J Roentgenol* 1995;165:645–646
5. Naganawa S, Ito T, Fukatsu H, et al. **MR imaging of the inner ear: Comparison of a three-dimensional fast spin-echo sequence with use of a dedicated Quadrature-surface phased array coil with a gadolinium-enhanced spoiled gradient recalled sequence.** *Radiology* 1998;208:679–685
6. Naganawa S, Itoh T, Fukatsu H, et al. **Three-dimensional fast spin-echo MR of the inner ear. Ultra-long echo train length and half Fourier technique.** *AJNR Am J Neuroradiol* 1998;19:739–741
7. Sartoretti-Schefer S, Kollias S, Wichmann W, Valavanis A. **T2-weighted three-dimensional fast spin-echo MR in inflammatory peripheral facial nerve palsy.** *AJNR Am J Neuroradiol* 1998;19:491–495
8. Czerny C, Rand T, Gstöttner W, et al. **MR imaging of the inner ear and cerebellopontine angle. Comparison of three-dimensional and two-dimensional sequences.** *AJR Am J Roentgenol* 1998;170:791–796